An application of the Dulmage-Mendelsohn partition to the analysis of a discretized dynamic chemical looping reactor model

Robert B. Parker [a], Chinedu O. Okoli [b,c], Bethany L. Nicholson [d], John D. Siirola [d], and Lorenz T. Biegler [a,1]

[a] Department of Chemical Engineering, Carnegie Mellon University, Pittsburgh, PA 15213

[b] National Energy Technology Laboratory, Pittsburgh, PA 15236

[c] NETL Support Contractor, Pittsburgh, PA 15236

[d] Center for Computing Research, Sandia National Laboratories, Albuquerque, NM 87123

Abstract

Full discretization of nonlinear differential-algebraic equation (DAE) systems is a popular approach for optimization of these systems due to the availability of general mathematical programming environments and nonlinear programming solvers, the fast solve times this approach may achieve, and its ability to handle constraints on state variables. The fully discretized DAE is a large-scale system of algebraic equations that may be handled efficiently by generic solvers. Due to its size, however, this system is not easy to analyze if an optimization solve fails to converge and a modeling error is suspected. To alleviate this difficulty, this work proposes to automatically partition a discretized DAE into differential and algebraic subsystems at each point in time and to apply a Dulmage-Mendelsohn partition to the bipartite graph of variables and equations of each of these subsystems. In this way, relatively small systems of equations can be analyzed for structural and numerical nonsingularity rather than the full, discretized DAE model. In the application to a chemical looping combustion reactor model from the IDAES process model library, the DAE model is found to have a structural singularity in the algebraic subsystems, and the Dulmage-Mendelsohn partition reveals the cause of this singularity. An updated version of the model is proposed to eliminate this singularity, and the performance of the two models in a dynamic optimization problem is compared.

Keywords

Differential-algebraic equations, discretization, graph theory, optimization

Introduction

Differential-algebraic equation systems (DAEs) are a versatile modeling tool for describing processes that evolve over time or space domains, and optimization problems involving DAEs are necessary for optimal control, state estimation, and parameter estimation of such systems. Simultaneous formulations of these optimization problems are popular for their fast solve times and ability to explicitly handle bounds on differential and algebraic state variables. Furthermore, tools built on generic algebraic modeling environments for automatic discretization and model construction facilitate the process of formulating optimization problems with discretized DAE models of chemical processes, and the underlying algebraic modeling environments allow these models to be sent to generic nonlinear optimization solvers. However, in the case that a solver fails to converge, we may want to validate the nonsingularity of our model equations and investigate for potential modeling errors. To investigate similar situations that arise in steady state process optimization, Bublitz et al. (2017) and Bunus and Fritzson (2002) suggest using the Dulmage-Mendelsohn partition (Dulmage and Mendelsohn (1958)) to identify overconstrained and underconstrained subsystems that may facilitate model debugging.

In addition, Shin et al. (2020) and Jalving et al. (2019) suggest using a "problem graph" for analysis and modular construction of graph-structured algebraic models, while Bynum et al. (2021) and Friedman et al. (2013) suggest using `Block` objects in Pyomo for the similar concept of hierarchically-structured models. These approaches facilitate algebraic model analysis and debugging by partitioning models into sub-models that can be analyzed individually.

We combine these two approaches, first partitioning the

[1] Corresponding author. Email: `biegler@cmu.edu`.

discretized DAE model into subsystems at each point in time, then applying the Dulmage-Mendelsohn partition to these subsystems for more targeted analysis than applying this partition to the full model would provide. We then apply this approach to a chemical looping combustion (CLC) reduction reactor in the IDAES process modeling framework to demonstrate its utility in identifying and fixing a singularity.

Background

DAE systems

A differential-algebraic equation system consists of differential and algebraic equations and differential, algebraic, and input variables x, y, and u, that are functions of a continuous domain. For convenience, we refer to this continuous domain as "time" and use an associated independent variable t which takes values between t_0 and t_f.

$$\left.\begin{aligned} 0 &= f(\dot{x}_t, x_t, y_t, u_t) \\ 0 &= g(x_t, y_t, u_t) \end{aligned}\right\} \quad t \in [t_0, t_f] \qquad (1)$$
$$x_{t_0} = \bar{x}_{t_0}$$

A discretized approximation of this DAE system is given in Equation (2). Here, t takes discrete values between t_0 and t_f with uniform spacing Δt. In this system, the time derivative $\dot{x}_{t_i}$ is approximated using a backward difference, or implicit Euler, discretization. The analysis in this work will assume an implicit Euler discretization, although similar analyses may be performed with other discretizations.

$$\left.\begin{aligned} 0 &= f(\dot{x}_t, x_t, y_t, u_t) && t \in \{t_0, \ldots, t_f\} \\ 0 &= g(x_t, y_t, u_t) && \\ \dot{x}_{t_i}\Delta t &= (x_{t_i} - x_{t_{i-1}}) && t_i \in \{t_1, \ldots, t_f\} \end{aligned}\right\} \qquad (2)$$
$$x_{t_0} = \bar{x}_{t_0}$$

A key property of DAE systems is the index-1 property. For the purpose of the analysis presented, we say that a DAE is *index-1* if the differential and algebraic Jacobian matrices $\nabla_{\dot{x}_t} f$ and $\nabla_{y_t} g$ are nonsingular everywhere. This property ensures that differential equations are sufficient to solve for the derivative variables $\dot{x}$ and that algebraic equations are sufficient to solve for algebraic variables (when treating all other variables as parameters). These properties are useful for demonstrating nonsingularity of the discretized DAE and are commonly made when creating a model of a process. This work focuses on verification of the index-1 property and treats its violation as a modeling error. More information on the DAE index property is given by Ascher and Petzold (1998).

Algebraic modeling environment

DAE systems representing chemical processes may be constructed and discretized with the help of several algebraic modeling tools. Pyomo.DAE (Nicholson et al. (2018)) allows the explicit creation of derivative variables and discretization equations in Pyomo (Bynum et al. (2021)), while the IDAES process modeling framework (Lee et al. (2021)) provides tools for constructing Pyomo.DAE models of chemical processes as well as a library of pre-defined unit models and thermophysical property packages. This work is concerned with the analysis of a chemical looping reduction reactor model from this library.

Bipartite graph of a discretized DAE

To analyze subsystems of a discretized DAE model for causes of singularity, we first treat the system as a bipartite graph in which one set of nodes corresponds to variables, the other set corresponds to equations, and there is an edge between a variable node and an equation node if the variable participates in the equation. A *maximum matching* attempts to pair as many equations and variables as possible such that no variable or equation is paired more than once. More formally, a *matching* in a graph is a set of disjoint pairs of adjacent nodes and a maximum matching is a matching with the largest possible cardinality. A maximum matching is a *perfect matching* if it contains every node. Neither a maximum matching nor a perfect matching is necessarily unique. If the maximum matching of the bipartite graph of a system of variables and equations is not a perfect matching, the Jacobian of this system is guaranteed to be singular. We refer to the Jacobian of a system that does not have a perfect matching as *structurally singular*. In this case, the Dulmage-Mendelsohn decomposition partitions the system into three subsystems: *Underconstrained*, where a maximum matching covers every equation but leaves unmatched variables, *overconstrained*, where a maximum matching covers every variable but leaves unmatched equations, and *square*, where a maximum matching is a perfect matching. An illustration of this decomposition for the reduction reactor model is given in Figure 2. This decomposition can provide significant insight into why a system is structurally singular. More information on these algorithms is given by Davis (2006).

Analysis of chemical looping combustion reactor

To demonstrate the utility of the tools and procedures described, we analyze the equations of a chemical looping reduction reactor obtained from IDAES version 1.7.

Model description

The reactor model we study is a dynamic instance of a reduction reactor in a chemical looping process described by Ostace et al. (2018) and Okoli et al. (2020). The reactor is a moving bed, counter-current reactor in which a methane fuel reacts with an iron oxide oxygen carrier according to the reaction (3). The moving-bed nature of the reactor informs the assumption that the solid phase moves with a velocity v_s, constant along the length of the reactor, that is less than the minimum fluidization velocity.

$$CH_4 + 12Fe_2O_3 \rightarrow 2H_2O + CO_2 + 8Fe_3O_4 \qquad (3)$$

The model is described by partial differential and algebraic equations, where states are defined over a time domain denoted by t and a spatial domain along the normalized length of the reactor denoted by z. The gas phase enters at $z = 0$ and flows in the positive z direction, while the solid phase enters at $z = 1$ and flows in the negative z direction. Degrees of

freedom are the flow rates and conditions of the gas and solid inlet flow streams. Flow rates are control inputs, while other inlet conditions may be treated as disturbances. For the purpose of the analysis in the remainder of this section, the reactor model is treated as a square system in which degrees of freedom are fixed. The nominal steady state operating conditions of this reactor correspond to inlet conditions with a gas flow rate of 128 mol/s, a solid flow rate of 591 kg/s, a gas composition of 97.5% CH_4 and 2.5% CO_2 by mole, a solid composition of 45% Fe_2O_3 and 55% Al_2O_3 by mass, and a pressure of 2.0 bar.

The differential equations are gas and solid phase material balances (4) and (5) and gas and solid phase energy balances (6) and (7).

$$l\frac{\partial M_i}{\partial t} = \frac{\partial f_i}{\partial z} + lN_{k,g},\ i \in \{CH_4, CO_2, H_2O\} \tag{4}$$

$$l\frac{\partial M_i}{\partial t} = \frac{\partial f_i}{\partial z} + lN_{i,s}\mathrm{MW}_i,\ i \in \{Fe_2O_3, Fe_3O_4, Al_2O_3\} \tag{5}$$

$$l\frac{\partial H_g}{\partial t} = \frac{\partial f_{H,g}}{\partial z} + lQ_g \tag{6}$$

$$l\frac{\partial H_s}{\partial t} = \frac{\partial f_{H,s}}{\partial z} - lQ_g + \Delta H_{\mathrm{rxn}}\xi \tag{7}$$

Here, $l = 5$ m is the length of the reactor, M_i is the material holdup of species i, f_i is the flow rate of i, $N_{i,g}$ is the rate of transport of i into the gas phase, $N_{i,s}$ is the rate of transport of i into the solid phase, MW_i is the molecular weight of i, H_g is the gas phase enthalpy holdup, H_s is the solid phase enthalpy holdup, $f_{H,g}$ is the gas phase enthalpy flow rate, $f_{H,s}$ is the solid phase enthalpy flow rate, Q_g is the rate of heat transfer into the gas phase, ξ is the extent of reaction, and ΔH_{rxn} is the enthalpy of reaction (3). Initial conditions are specified in terms of material and energy holdups along the length domain.

Algebraic equations describe thermodynamics, reactions, and transport within the reactor model. Selected algebraic equations that are necessary for the analysis in the remainder of this section are the gas and solid holdup equations (8) and (9), the skeletal and particle density equations (10) and (11), the gas and solid area equations (13) and (12), the gas and solid component sum equations (14) and (15), the solid component flow equation (16), and the solid enthalpy flow equation (17).

$$M_i = \rho_g y_i A_g,\ i \in \{CH_4, CO_2, H_2O\} \tag{8}$$

$$M_i = \rho_{\mathrm{ptcl}} x_i A_s,\ i \in \{Fe_2O_3, Fe_3O_4, Al_2O_3\} \tag{9}$$

$$\rho_{\mathrm{skel}} = \left(\sum_{i \in \{Fe_2O_3, Fe_3O_4, Al_2O_3\}} \frac{x_i}{\rho_{\mathrm{skel},i}} \right)^{-1} \tag{10}$$

$$\rho_{\mathrm{ptcl}} = (1 - \varepsilon_{\mathrm{ptcl}})\rho_{\mathrm{skel}} \tag{11}$$

$$A_s = (1 - \varepsilon)A \tag{12}$$

$$A_g = \varepsilon A \tag{13}$$

$$\sum_{i \in \{CH_4, CO_2, H_2O\}} y_i = 1 \tag{14}$$

$$\sum_{i \in \{Fe_2O_3, Fe_3O_4, Al_2O_3\}} x_i = 1 \tag{15}$$

$$f_i = x_i F_s,\ i \in \{Fe_2O_3, Fe_3O_4, Al_2O_3\} \tag{16}$$

$$f_{H,s} = \hat{H}_s F_s \tag{17}$$

In these equations, ρ_g is the gas phase molar density, ρ_{ptcl} is the density of the porous solid particle, ρ_{skel} is the density of the solid material, $\rho_{\mathrm{skel},i}$ is the density of species i, y_i is a gas phase mole fraction, x_i is a solid phase mass fraction, $\varepsilon_{\mathrm{ptcl}}$ is the particle porosity, $A = 33.2\ \mathrm{m}^2$ is the reactor cross-sectional area, A_g and A_s are the cross-sectional areas occupied by the gas phase and solid particles, $\varepsilon = 0.8$ is the bed void fraction, and F_s is the solid phase mass flow rate.

The model is discretized with Pyomo.DAE using a backward difference discretization in the time domain, a backward difference discretization for the gas phase spatial derivatives, and a forward difference discretization for the solid phase spatial derivatives. In the instance of this model used for the following analysis, a 300 s horizon with 11 discretization points is used. Eleven discretization points are used for the normalized length domain as well. The full model equations, including values of all parameters used, may be found in the `idaes/gas_solid_contactors` directory in version 1.7 of the IDAES repository at `github.com/idaes/idaes-pse`. With the reactor model defined, we would like to analyze the equations to identify singularities and their causes. The analysis for the remainder of this section considers the discretized process model with degrees of freedom fixed to nominal values. In this way, the discretized model is a square system of variables and equations that can be partitioned and analyzed with the Dulmage-Mendelsohn decomposition.

Model analysis

We first partition the model into square subsystems at each point in the discretized time domain and analyze each for singularity by performing a maximum matching. The corresponding decomposition of the Jacobian matrix is given by Equation (18), where J is the Jacobian of the discretized DAE and J_t is the Jacobian of the subsystem of equations and variables at time point t. The incidence matrix of the discretized reactor model is shown in the left half of Figure 1. Here and throughout, rows correspond to equation coordinates and columns correspond to variable coordinates. The system portrayed has 10,197 equations and variables.

$$J = \begin{bmatrix} J_{t_0} & & \\ * & \ddots & \\ * & * & J_{t_f} \end{bmatrix} \tag{18}$$

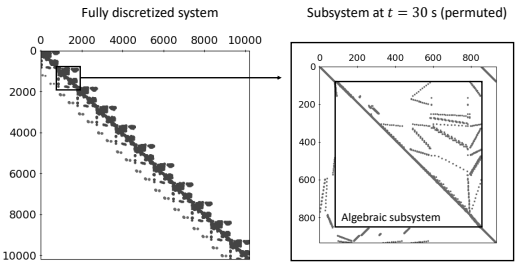

Figure 1: Left: Incidence matrix of variables and equations in the discretized chemical looping model. Right: Subsystem at $t = 30$ s permuted into the order given by Equation (19).

Performing a maximum matching on the variables and equations of this system reveals a singularity as the cardinality of the maximum matching is only 10,187 – there are 10 unmatched variables and equations. Rather than analyze the incidence graph of the full, discretized system, however, we break this system down into discretization, differential, and algebraic subsystems at each point in time and analyze these smaller systems individually. The corresponding partition of the Jacobian submatrix at time t is shown in Equation (19).

$$J_t = \begin{bmatrix} I & & -\Delta t I \\ \nabla_{x_t} g_t & \nabla_{y_t} g_t & \\ \nabla_{x_t} f_t & \nabla_{y_t} f_t & \nabla_{\dot{x}_t} f_t \end{bmatrix} \tag{19}$$

We note that nonsingularity of $\nabla_{y_t} g_t$ and $\nabla_{\dot{x}_t} f_t$ is sufficient for structural nonsingularity of J_t, and for numerical nonsingularity of J_t in the limit as $\Delta t \to 0$. The incidence matrix of the reactor model at $t = 30$ s, permuted into the order given by Equation (19), is shown in the right half of Figure 1. This partition of equations and variables is obtained by identifying the modeling components introduced by Pyomo.DAE.

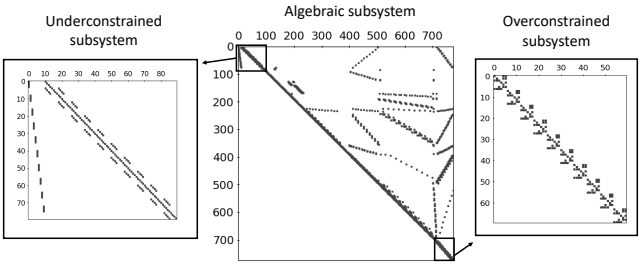

Figure 2: Center: Incidence matrix of algebraic subsystem at $t = 30$ s with variables and equations ordered according to the Dulmage-Mendelsohn partition. Left: Incidence matrix of the underconstrained subsystem. Right: Incidence matrix of the overconstrained subsystem, permuted into independent diagonal blocks.

The Jacobian of discretization equations with respect to differential variables M_i, H_g, and H_s and that of differential equations (4)-(7) with respect to time derivative variables are nonzero multiples of the identity matrix, and are therefore nonsingular. A maximum matching of the rows and columns of the algebraic Jacobian $\nabla_{y_t} g_t$, however, reveals that it is singular. In the Dulmage-Mendelsohn partition, the underconstrained system contains 90 variables and 80 equations, while the overconstrained system contains 60 variables and 70 equations. The incidence matrix of the algebraic subsystem at $t = 30$ s, $\nabla_{y_{t_1}} g_{t_1}$, is shown in the center of Figure 2, permuted into an order consistent with the Dulmage-Mendelsohn partition. We would like to identify the cause of this singularity by examining the equations and variables in the overconstrained and underconstrained subsystems.

The incidence matrix of the overconstrained subsystem is shown in the right third of Figure 2. The rectangular diagonal blocks in this incidence matrix each contain variables and equations at a particular point in the discretized length domain. The variables are the solid phase mass fractions $x_{Fe_2O_3}$, $x_{Fe_3O_4}$, and $x_{Al_2O_3}$, the solid phase skeletal density ρ_{skel}, the solid phase particle density ρ_{part}, and the solid phase cross-sectional area A_s at a particular point in the length domain. The equations are the holdup calculation equations (9), the particle density equation (11), the skeletal density equation (10), the solid phase area equation (12), and the mass fraction sum equation (15).

Among these equations, we would expect the mass fraction sum equation to be matched with one of the mass fraction variables and for the particle density variable to be matched with the corresponding holdup calculation equation. In this case, the particle density equation would be unmatched, but could be matched with particle porosity if it were made a variable indexed by space and time rather than a constant parameter. Letting particle porosity vary also makes the model more realistic, as the assumption of constant particle porosity does not necessarily hold for a reacting solid. Adding this variable yields a system with more variables than constraints, so in this case an equation must be added to make sure the algebraic subsystem remains square. To determine what equation should be added or variable fixed, we examine the underconstrained subsystem, the incidence matrix of which is shown in the left third of Figure 2.

The underconstrained subsystem does not admit a partition into independent diagonal blocks; however, by inspection, it contains the same nine variables and eight equations, repeated at every point in the discretized spatial domain except for the solid inlet at $z = 1$. These variables are the total solid phase flow rate F_s, the solid phase component flow rates $f_{Fe_2O_3}$, $f_{Fe_3O_4}$, and $f_{Al_2O_3}$, the solid enthalpy flow rate $f_{H,s}$, the solid material flow gradients $\frac{df_{Fe_2O_3}}{dz}$, $\frac{df_{Fe_3O_4}}{dz}$, and $\frac{df_{Al_2O_3}}{dz}$, and the solid enthalpy flow gradient $\frac{df_{H,s}}{dz}$. The equations are the solid phase material and enthalpy flow equations (16) and (17) and the material and enthalpy gradient discretization equations. Among the variables in this overconstrained subsystem, all are well-determined by these equations other than the solid phase total flow rate F_s. Because the velocity v_s, particle density, and cross-sectional area of the solid phase is known, this flow rate is known as well by Equation 20.

$$F_s = \rho_{part} A_s v_s \tag{20}$$

However, this equation is not included in the chemical looping reactor model as of IDAES 1.7. To calculate the solid flow rate F_s and keep the algebraic system square while we make particle porosity a variable, we propose adding Equation (20), the solid flow-density equation, to the reactor model at every point in the discretized length domain. We refer to the new version of the reactor model, with these changes made, as the "patched version" of the model.

After adding Equation (20) to the moving bed reactor model, we may repeat the incidence matrix analysis to make sure the square model is now nonsingular. The discretized system now has 10,310 variables and equations. A maximum matching of this system has cardinality 10,310, indicating that the system is structurally nonsingular. In addition, we may analyze the algebraic subsystem at every point in time. The incidence matrix of the subsystem at $t = 30$ s, as well as the isolated algebraic subsystem, is shown in Figure 3.

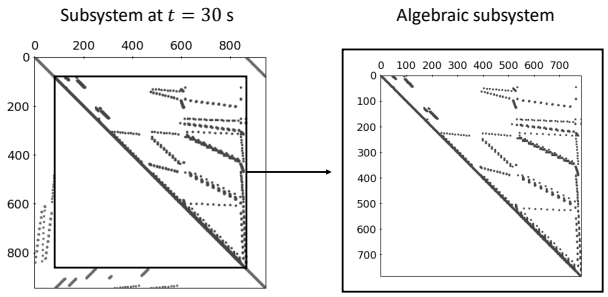

Figure 3: Left: Incidence matrix of the subsystem of the patched reactor model at $t = 30$ s. Right: Incidence matrix of the algebraic subsystem, permuted to block triangular form.

The algebraic subsystem at a particular point in time in the patched model has 785 equations and variables. In contrast to the algebraic subsystem of the old model, the incidence matrix of which is shown in Figure 2, the incidence matrix of the patched algebraic subsystem may be permuted to have a zero-free diagonal and is structurally nonsingular. One particular permutation with a zero-free diagonal, that of a block lower triangular form, is shown in Figure 3. This system has a trivial Dulmage-Mendelsohn partition as the underconstrained and overconstrained subsystems are empty – the algebraic system is now structurally well-determined.

A block triangularization of the algebraic subsystem of the patched model yields an ordered partition into 665 square diagonal blocks, only 40 of which have more than one variable and equation. Evaluated at the nominal steady state of the reactor model, none of the blocks have an all-zero Jacobian. For the 40 blocks with more than one variable and equation, the maximum condition number is 2×10^6, so this algebraic Jacobian is both structurally and numerically nonsingular at the point evaluated.

Comparison of old and new models

With the singularity in the algebraic subsystem eliminated, we would like to check whether the model performs better for the purpose of dynamic optimization. To this end, we pose a dynamic optimization problem involving the reactor model, construct the KKT matrix of this optimization problem, and attempt to solve the optimization problem with IPOPT 3.13.2 with the old and new versions of the model.

The dynamic optimization problem that we pose seeks to minimize deviation from a target setpoint, given an initial setpoint as initial conditions. Control inputs are gas and solid inlet flow rates, which are piecewise constant on 60 s intervals. The variables fixed at $t = 0$ as initial conditions are gas phase material and energy holdups M_{CH_4}, M_{CO_2}, M_{H_2O}, and H_g at all points in space except the gas inlet at $z = 0$ and solid phase material and energy holdups $M_{Fe_2O_3}$, $M_{Fe_3O_4}$, $M_{Al_2O_3}$, and H_s at all points in space except the solid inlet at $z = 1$. Collectively, these variables whose initial conditions are fixed are referred to as v, with initial values $\bar{v}_0$ obtained from the initial steady state. The variables with deviation-from-setpoint penalized in the objective function are gas flow rate f_g, solid flow rate f_s, pressure P, gas mole fractions y_{CH_4}, y_{H_2O}, and y_{CO_2}, solid mass fractions $x_{Fe_2O_3}$, $x_{Fe_3O_4}$, and $x_{Al_2O_3}$, gas temperature T_g, and solid temperature T_s. Again, these states are penalized at all points in space except for the inlet of their respective phases. Collectively, these variables penalized in the objective are referred to as w, with target values w^* obtained from a target steady state. In the instance of this problem used for this comparison, the initial steady state is the nominal steady state described above. The target steady state is the steady state corresponding to the same inlet parameters for pressure, composition, and temperatures, but with a gas inlet flow rate of 140 mol/s and a solid inlet flow rate of 600 kg/s. Variables in the optimization problem are initialized to their values at the initial steady state. The formulation of this optimization problem is given by Problem (21). We formulate and attempt to solve this optimization problem with the original and patched versions of the reduction reactor model.

$$\begin{array}{ll} \min & \sum_t \|w_t - w^*\|^2 \\ \text{s.t.} & \text{Discretized model equations} \\ & F_g \text{ and } F_s \text{ piecewise constant} \\ & v_0 = \bar{v}_0 \end{array} \tag{21}$$

We note that Problem (21) is an equality-constrained optimization problem and can be solved by applying a globalized Newton method to the optimality conditions of this equality-constrained problem (Nocedal and Wright (2006)). One of the requirements to guarantee convergence is that the Jacobian of the system of optimality conditions is nonsingular. This Jacobian, K, is given by Equation (22), where W is the Hessian of the Lagrangian of Problem (21) and A is the Jacobian of the equality constraints.

$$K = \begin{bmatrix} W & A \\ A^T & \end{bmatrix} \tag{22}$$

We would like to check whether this matrix is singular for Problem (21), evaluated at the initial guess (variables take their initial steady state values), with the original and patched versions of the model used in the equality constraints. To check singularity, we perform a symbolic and numerical factorization with MA27 (Duff and Reid (1982)), as this code is commonly used in optimization solvers. In addition, we attempt to solve each optimization problem with IPOPT (Wächter and Biegler (2006)), using MA27 as the linear solver. The results of factorizing the K and solving the optimization problem are given in Table 1.

Table 1: Statistics of the dynamic optimization problem with two versions of the reduction reactor model

Model	Rank	Max. reg. coef.	Iterations
Original	20,417 / 20,430	7.8	N/A
Patched	20,650 / 20,650	N/A	4

In Table 1, the rank is reported as a fraction of the row/column dimension. "Max. reg. coef." refers to the maximum regularization coefficient used by IPOPT to try to converge despite a singular KKT matrix (see Wächter and Biegler (2006)). Iterations are the number of iterations required for a successful convergence. These results indicate that the K with the original model is singular, while K with the patched model is nonsingular. Furthermore, the optimization problem with the patched model converges quickly and without regularization, while that with the original model terminates after with diverging iterates.

Conclusion

We have presented an approach for analyzing a discretized DAE model in which we first exploit knowledge of problem structure to partition the variables and equations into differential, algebraic, discretization, and derivative at each point in time, then use the Dulmage-Mendelsohn partition to analyze these subsystems individually and identify the cause of singularities. We have applied the approach to a chemical looping combustion reactor model in IDAES 1.7 to find and eliminate singularities in a patch incorporated as of IDAES 1.8. The patched version of the model leads to a nonsingular KKT matrix and fast convergence in a simple optimization problem that does not converge otherwise. This study demonstrates the advantage of combining knowledge of problem structure with analyses of the bipartite graphs of specially identified subsystems. Furthermore, the comparison of the dynamic optimization problem with the two models illustrates the importance of eliminating singularities in the model Jacobian. The Dulmage-Mendelsohn partition has been implemented in Pyomo and may be accessed in the `pyomo/contrib/incidence_analysis` subdirectory of the Pyomo repository at `github.com/pyomo/pyomo`. Code used to produce the included results may be found at `github.com/IDAES/publications`. We hope this work will serve as an illustrative example of a systematic procedure to identify the causes of singularity in large-scale, structured, nonlinear algebraic models.

Disclaimer: This project was funded by the United States Department of Energy, National Energy Technology Laboratory, in part, through a site support contract. Neither the United States Government nor any agency thereof, nor any of their employees, nor the support contractor, nor any of their employees, makes any warranty, express or implied, or assumes any legal liability or responsibility for the accuracy, completeness, or usefulness of any information, apparatus, product, or process disclosed, or represents that its use would not infringe privately owned rights. Reference herein to any specific commercial product, process, or service by trade name, trademark, manufacturer, or otherwise does not necessarily constitute or imply its endorsement, recommendation, or favoring by the United States Government or any agency thereof. The views and opinions of authors expressed herein do not necessarily state or reflect those of the United States Government or any agency thereof.
Sandia National Laboratories is a multimission laboratory managed and operated by National Technology and Engineering Solutions of Sandia, LLC., a wholly owned subsidiary of Honeywell International, Inc., for the U.S. Department of Energy's National Nuclear Security Administration under contract DE-NA-0003525. This paper describes objective technical results and analysis. Any subjective views or opinions that might be expressed in the paper do not necessarily represent the views of the U.S. Department of Energy or the United States Government. SAND2022-9098 C.

References

Ascher, U. M. and L. R. Petzold (1998). *Computer methods for ordinary differential equations and differential algebraic equations*.

Bublitz, S., E. Esche, G. Tolksdorf, V. Mehrmann, and J.-U. Repke (2017). Analysis and decomposition for improved convergence of nonlinear process models in chemical engineering. *Chemie Ingenieur Technik 89*(11), 1503–1514.

Bunus, P. and P. Fritzson (2002). Methods for structural analysis and debugging of modelica models. In *Proceedings of the 2nd International Modelica Conference*, Oberpfaffenhofen, Germany, pp. 157–165.

Bynum, M. L., G. A. Hackebeil, W. E. Hart, C. D. Laird, B. L. Nicholson, J. D. Siirola, J.-P. Watson, and D. L. Woodruff (2021). *Pyomo–optimization modeling in python* (Third ed.), Volume 67. Springer.

Davis, T. A. (2006). *Direct Methods for Sparse Linear Systems*. SIAM.

Duff, I. S. and J. K. Reid (1982). MA27 – A set of Fortran subroutines for solving sparse symmetric sets of linear equations. Technical Report AERE-R 10533, AERE Harwell.

Dulmage, A. L. and N. S. Mendelsohn (1958). Coverings of bipartite graphs. *Can. J. Math.*, 517–534.

Friedman, Z., J. Ingalls, J. D. Siirola, and J.-P. Watson (2013). Block-oriented modeling of superstructure optimization problems. *Comp. Chem. Eng. 57*, 10–23.

Jalving, J., Y. Cao, and V. M. Zavala (2019). Graph-based modeling and simulation of complex systems. *Comp. Chem. Eng. 125*, 134–154.

Lee, A., J. H. Ghouse, J. C. Eslick, C. D. Laird, J. D. Siirola, M. A. Zamarripa, D. Gunter, J. H. Shinn, A. W. Dowling, D. Bhattacharyya, L. T. Biegler, A. P. Burgard, and D. C. Miller (2021). The IDAES process modeling framework and model library–Flexibility for process simulation and optimization. *J. Adv. Manuf. Proc. 3*(3), e10095.

Nicholson, B., J. D. Siirola, J.-P. Watson, V. M. Zavala, and L. T. Biegler (2018). `pyomo.dae`: A modeling and automatic discretization framework for optimization with differential and algebraic equations. *Math. Prog. Comp. 10*(2), 187–223.

Nocedal, J. and S. J. Wright (2006). *Numerical Optimization*. Springer.

Okoli, C. O., A. Ostace, S. Nadgouda, A. Lee, A. Tong, A. P. Burgard, D. Bhattacharyya, and D. C. Miller (2020). A framework for the optimization of chemical looping combustion processes. *Powder Technology*, 149–162.

Ostace, A., A. Lee, C. O. Okoli, A. P. Burgard, D. C. Miller, and D. Bhattacharyya (2018). Mathematical modeling of a moving-bed reactor for chemical looping combustion of methane. In *Proc. 13th Int. Sympos. PSE*, Comp.-Aid. Chem. Eng., pp. 325–330. Elsevier.

Shin, S., C. Coffrin, K. Sundar, and V. M. Zavala (2020). Graph-based modeling and decomposition of energy infrastructures. *arXiv preprint arXiv:2010.02404*.

Wächter, A. and L. T. Biegler (2006). On the implementation of an interior-point filter line-search algorithm for large-scale nonlinear programming. *Math. Prog.*, 25–27.